
iMold: Enabling Interactive Design Optimization for In-Mold Electronics

Jonathan Ting¹

University of California Berkeley
Berkeley, CA, USA
jkting4@berkeley.edu

James D. Holbery¹

Tactual Labs
Redmond, WA, USA
holbery@yahoo.com

Yunbo Zhang

Rochester Institute
of Technology
Rochester, NY 14623, USA
ywzeie@rit.edu

Siyuan Ma

Applied Sciences, Microsoft
Redmond, WA, USA
siyma@microsoft.com

Sang Ho Yoon

Applied Sciences, Microsoft
Redmond, WA, USA
sayoon@microsoft.com

¹Work done while the author was at Microsoft.

Permission to make digital or hard copies of part or all of this work for personal or classroom use is granted without fee provided that copies are not made or distributed for profit or commercial advantage and that copies bear this notice and the full citation on the first page. Copyrights for third-party components of this work must be honored. For all other uses, contact the owner/author(s).
CHI '20 Extended Abstracts, April 25–30, 2020, Honolulu, HI, USA.
© 2020 Copyright is held by the author/owner(s).
ACM ISBN 978-1-4503-6819-3/20/04.
<http://dx.doi.org/10.1145/3334480.3382804>

Abstract

In recent years, in-mold electronics (IME) technique was introduced as a combination of printing electrically functional materials and vacuum plastic forming. IME has gained significant attention across various industries since it enables various electrical functionalities on a wide range of 3D geometries. Although IME shows great application potentials, hardships still exist during design for the manufacturing stage. For example, printed 2D structures experience mechanical bending and stretching during vacuum forming. This results in challenges for designers to ensure precise circuit-to-3D mold registration or to prevent over deformation of circuit and attached components. To this end, we propose a software toolkit that provides real time 2D-to-3D mapping, guided structural and electrical circuit design with interactive user interface. We present a novel software-guided IME process that leads to fully functional 3D electronic structures with printed conductive traces and assembled surface-mount components.

Author Keywords

In-Mold Electronics, Design Tool, Flexible Electronics

CCS Concepts

•Human-centered computing → *Interactive systems and tools;*

Introduction

In-mold electronics (IME) manufacturing is a process of a combination of traditional plastic molding and functional materials printing, which shows great potential in creating various human machine interfaces. IME enables creating of interactive 3D objects at large scale, where high market value is predicted [6]. Recent advancements of electronic inks have further matured the development of IME. For example, some recently developed advanced ink systems are both electrically conductive with capability of enduring significant mechanical elongation during forming process under vacuum. However, the overall IME fabrication process is challenging. For instance, the printed substrate is heated above its melting temperature during forming process and the pre-patterned conductive traces bend and stretch along with the molten substrate relative to the applied 3D mold. No design tool exists to ensure precise registration between printed patterns to 3D molds. Moreover, there is lack of a standard design strategies to prevent over deformation of printed circuits. In this work, we propose a software toolkit as a design assistance enabling interaction design with mechanical and electrical optimizations for IME. In this work, we present *iMold* that renovates standard IME in two-fold: (1) offering an universal design guidance software toolkit where users can optimize printing screen design from a given 3D geometry and (2) establishing a full IME process including component assembly by adding an automatic surface-mounting process in-between printing and vacuum forming. This allows us to reduce design iterations during manufacturing and enable a wide range of electronic functionalities while supporting production scalability.

Related Works

IME is under active development among various fields. For instance, the chemical industry [2, 5, 11] is actively devel-

oping conductive inks and component connection materials for IME processes. There are a few companies [1, 3, 4, 12] putting efforts on IME manufacturing process and infrastructure development. Furthermore, state-of-art research works have shown the potential of adopting IME for organic light emitting devices (OLED), LED, touch panel and electrochromic displays [7, 8, 10]. In the thermoforming process, the 2D textures are often transformed onto 3D shapes with a dramatic deformation. It is a challenging task to design the 2D textures interpolating onto 3D shapes without undesired pattern distortion. Previously, researchers tackled this problem from the perspective of computational geometry [13, 16]. Schüller et al. [13] considered the thermoforming process as a texture mapping, and established the 2D-to-3D correspondence to predict the shape distortion incurred from the process. Based on the predicted shape distortion, a pre-distorted texture is computed to compensate the shape distortion. Differently, Zhang et al. [13] employed a physical simulation to establish the shape distortion prediction during the thermoforming process, and employed this prediction to correct the designed 2D textures.

In the previous works, the in-mold electronics fabrication process developments are solely based on iterations of trial and error identification. Specially, printing screens were designed at first place with no considerations of 3D mold geometrical challenges. Then a few iterations of screen redesign are needed based on detecting and preventing of mechanical and electrical failure locations. These interactions inevitably involve high cost of trained labor, time and materials. A software-guided design interface for in-mold electronics printing screen design is in need of minimizing the shape distortion. The limited software effort of relevant research is only focused on non-electrical cosmetic patterns. Although 2D to 3D mapping of cosmetic patterns is inspiring for in-mold electronics process design, it does not



Figure 1: Proposed In-mold Electronics fabrication process.

fully solve the need of in-mold electronics due to low tolerance requirement of shape distortion with considerations from failure probabilities from both mechanical and electrical engineering perspectives. In this work, we focus on generating electronic circuit patterns with customizable functionalities. We propose the software system that contains a set of interactive tools for customizing the semi-automatic conductive trace generation with minimized trace distortion during vacuum forming based on arbitrarily input 3D molds, automatic trace conductivity prediction prior and after vacuum forming and surface-mount component placement location recommendations. To the best of our knowledge, iMold- a comprehensive software interface is reported for the first time which enables a fully guided-design process of in-mold electronics printing screen design.

Screen Printing

On $12 \times 12 \times 1/8$ " Polyethylene terephthalate (PETG) substrates (McMaster Carr), conductive silver ink (Dupont ME603) was deposited using screen printing process (Ekra Semi-Automatic Screen and Stencil Printer E2) (Figure 1). Dupont ME603 was selected for its high conductivity and mechanical durability under thermoforming conditions. Subsequent to screen printing, the ink patterns were thermally treated at 70°C for 2 hours.

iMold Process Overview

Component Surface Mounting& Encapsulation

To attach the solid-state components to the printed PETG substrates, a standard pick-and-place process was used. Here, we used a multi-purpose die bonder (Finetech FINEPLACER[®] pico ma). By replacing the pick-and-place tip with a needle, small drops of bonding material were then transferred by sharp pins onto desired locations.

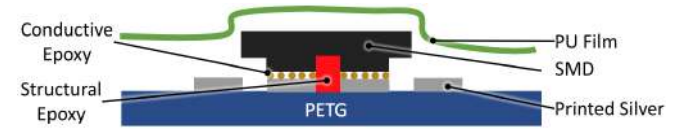


Figure 2: IME structure with printed traces, conductive adhesive, structural adhesive, and encapsulation from cross-sectional view.

Two different bonding materials were placed before pick-and-placing the solid-state components: (1) Loctite 3621 structural epoxy in the center between the two printed pads, and (2) Dupont ME902 conductive silver-embedded epoxy on each printed pad. The overall layer structure is shown in Figure 2.

The conductive silver epoxy serves as the electrical and mechanical connection between the surface mount devices (SMD) metal pads and the printed silver pattern on substrate. The non-conductive structural adhesive further improves the mechanical adhesion. After pin-transferring these two materials, SMDs were transferred on desired locations. The structures were then cured for 2 hours at 70°C and a polyurethane film from Dupont Intexar is laminated at an elevated temperature of 120°C over the surface of the SMDs, which serves as protective coating. It is worth noting that previous works involve manually manipulating components subsequent to vacuum forming process, which prevents process scalability. However surface mounting strategy developed and applied in this work (with assistance of our software design-aid kit) happens prior 3D forming step, which enables potential automatic component bonding at large manufacturing scale.

Vacuum Forming

In this work, we used an industrial standard thermoforming machine (Formech 686PT). The machine is preheated

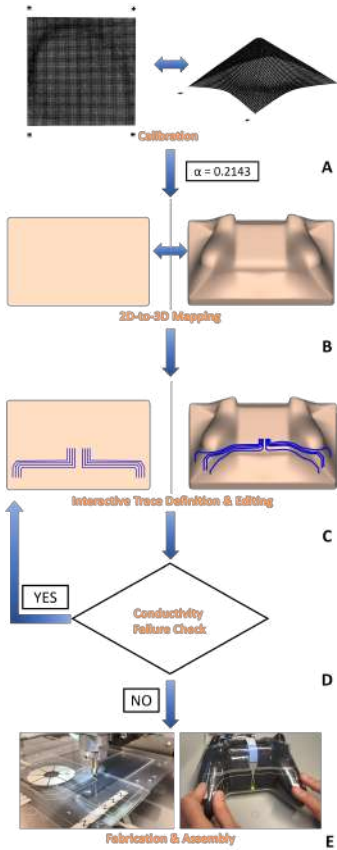


Figure 3: The workflow of the Software Toolkit consists of a calibration for material dependent shape parameter α (shown in A), the computation of 2D-to-3D mapping (B), the interactive trace definition and editing (C), and the conductivity failure detection (D). The completed design is then sent to fabrication (see E).

at 70% power for 20 minutes before starting any process. After the substrate and mold have been loaded, the heat cycle is performed at 70% for 80 seconds, and samples are cooled in ambient for 20 seconds before removing the formed part from the mold.

Computational Design Toolkit

We developed a computational design toolkit for interactively customizing the functional electronics patterns and detecting conductivity failures (See the workflow shown in Figure 3). Similar to [13], we establish a mapping between the 2D printed substrate and the 3D formed shape via a geometry based simulation (Figure 3(B)). In order to obtain a material dependent shape parameter involved in the mapping, we conducted a calibration onto preset test mold (Figure 3(A)). The shape parameter will remain the same if the substrate material is determined. With the established mapping, we provided the users a set of interactive tools for placing connectors and semi-automatically generating the traces linking pins of connectors (Figure 3(C)). Another important function we provided is the conductivity failure detection (Figure 3(D)). Since the large distortion introduced in the regions with high curvature during the forming, the conductivity of the traces in these regions could be increased dramatically to a failure, it is important to detect such failure and notify users to make adjustment to the trace.

2D-to-3D Mapping

The computation of the 2D-to-3D mapping is similar to the state-of-art surface parameterization problem [9], which aims to figure out the one-to-one correspondence of any position on the 3D surface and the 2D pattern.

In general, the 2D-to-3D mapping will have distortion introduced due to most of the 3D surface is not developable.

Therefore, computing 2D-to-3D mapping is to find a solution to an optimization problem, in which the distortion of mapping is formulated in certain forms (e.g. surface area difference, shape difference, and etc.). The method we adopted in this paper is inspired by [9], which presents a local/global approach for 3D regular surface parameterization. In their paper, an “as-rigid-as-possible” objective function and an “as-similar-as-possible” objective are formulated to represent different types of parameterization. Optimizing “as-rigid-as-possible” objective function minimizes the surface area difference between the 3D surface and its corresponding 2D pattern, while optimizing “as-rigid-as-possible” objective minimizes the shape difference. Figure 4 (a) and (b) show the different effect of satisfying “as-rigid-as-possible” objective and satisfying “as-similar-as-possible” objective respectively. On each triangle t_D on 2D pattern D , stratifying “as-rigid-as-possible” objective in the 2D-to-3D mapping can be considered as only applying the a rotation matrix \mathbf{R}_t to t_D to have a 3D triangle t_S on 3D surface S . Similarly, stratifying “as-rigid-as-possible” objective for each individual triangle t_D is to apply a scaling matrix \mathbf{W}_t to t_D . Instead of solely applying \mathbf{R}_t or \mathbf{W}_t , the 2D-to-3D mapping in thermoforming process requires applying the combination of rotation and scaling to each of the triangle, and therefore, a new transformation matrix \mathbf{T} is defined as

$$\mathbf{T}_t = (1 - \alpha) \cdot \mathbf{R}_t + \alpha \cdot \mathbf{W}_t, \quad (1)$$

where α is scalar shape parameter to control to how much the shape distortion will be introduced in the forming process. In order to control the resultant transformation matrix \mathbf{T}_t varies between \mathbf{R}_t and \mathbf{W}_t , we used the unified weight, which are α and $1 - \alpha$, and their summation is always 1. The physical meaning of α is a material dependent parameter, while α tends to 0 represents more rigid material and α tends to 1 means more soft material. To obtained α for certain material, we conduct a calibration, which is detailed

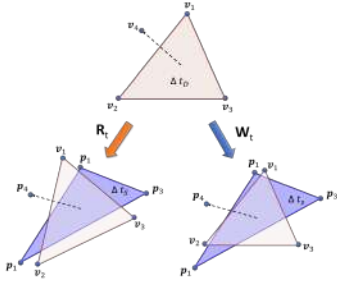


Figure 4: For a given triangle t_D on the 2D substrate to be mapped its 3D counterpart t_S on formed 3D surface S , applying only the rotational transformation will lead to a shape shown on the left, and applying only the scaling transformation will lead to a shape on the right.

in the next section. Both \mathbf{R}_t and \mathbf{W}_t can be computed with the three vertices of triangle t_D on D and the vertices of t_S on S using a *Singular Value Decomposition* (SVD). For the details of computing \mathbf{R}_t and \mathbf{W}_t , please refer to [9]. The combined transformation matrix \mathbf{T}_t is considered as the target transformation for each of the triangle t during the forming process. The actual transformation \mathbf{X}_t is expected to follow the target \mathbf{T}_t , and can be computed by minimizing the objective function $E_{mapping}$ as follows:

$$E_{mapping} = \sum_{t=1}^{f_n} \|\|\mathbf{X}_t - \mathbf{T}_t\|\|_F^2, \quad (2)$$

where f_n is the total number of the triangles on D , \mathbf{T}_t is the target transformation matrix for triangle t , \mathbf{X}_t is the unknown transformation matrix for t , and the $\|\|\cdot\|\|_F$ is the *Frobenius norm*. As $E_{mapping}$ is in the quadratic form, this optimization problem can be solved as a linear *Least-Square Problem* by solving a series of linear equations. Again, the details of solving Eq. 2 can be found in [9].

Calibration

To assess the shape parameter α , we borrowed the idea of [13] and conducted calibration forming tests. One test mold was a pyramid structure, and one was a hemisphere structure. A 1mm x 1mm square grid was printed onto PETG with the same silver ink used in the previous manufacturing process. The printed grid was scanned with a 3D scanner before and after thermoforming onto one of the calibration molds (See Figure 3(A)). With the scanned 2D substrate data and the 3D formed data, we are able to compute the α from them. The computed $\alpha = 0.2143$ is fixed and used throughout all the tested examples.

Interactive Trace Generation

Based on the 2D-to-3D mapping, we developed a sequence of interactive tools for user to define traces on the 2D substrate and preview the resultant 3D traces simultaneously. we adopt the *styling curve* [14, 15] as the representation of traces. The styling curve consists of a series of *attribute node* with not only position information and the triangular mesh connectivity information on the D . Since the triangular mesh connectivity of S is same as the one of D , the defined styling curve can be instantaneously mapped onto S . There are two different types of the attribute node, the *attribute edge node* \mathbf{p}_{edge} and the *attribute face node* \mathbf{p}_{face} . Therefore, the position of \mathbf{p}_{edge} can be calculated by interpolating the two end points ($\mathbf{p}_1, \mathbf{p}_2$) of a triangular edge with a parameter $u \in [0, 1]$: $\mathbf{p}_{edge} = (1 - u) \cdot \mathbf{p}_1 + u \cdot \mathbf{p}_2$. Similarly, an attribute face node is associated with a triangular facet with the barycentric coordinates (u, v, w) , where $u, v, w > 0$ and $u + v + w = 1$. Also, its 3D position is calculated by interpolating the three vertices ($\mathbf{p}_1, \mathbf{p}_2$, and \mathbf{p}_3) of the triangular facet: $\mathbf{p}_{face} = u\mathbf{p}_1 + v\mathbf{p}_2 + w\mathbf{p}_3$. Once the styling curve is defined on 2D substrate, a 3D curve is obtained instantaneously based on the established 2D-to-3D mapping.

Built upon the styling curves attribute nodes, we developed the curve creation and editing tools. Via the mouse left clicks, a set of points are picked as the control points. These control points are used to generate a smooth curve automatically by interpolating these picked control points via the *four-points interpolation* scheme as follows:

$$\mathbf{c}_i^* = -\frac{1}{16}\mathbf{c}_{i-1} + \frac{9}{16}\mathbf{c}_i + \frac{9}{16}\mathbf{c}_{i+1} - \frac{1}{16}\mathbf{c}_{i+2}, \quad (3)$$

where \mathbf{c}_{i-1} , \mathbf{c}_i , \mathbf{c}_{i+1} , and \mathbf{c}_{i+2} are the four sequencing control points, and \mathbf{c}_i^* is the newly generated points. Then, \mathbf{c}_i^* is inserted between \mathbf{c}_{i-1} and \mathbf{c}_i . After repeating the four-points interpolation several times, more and more

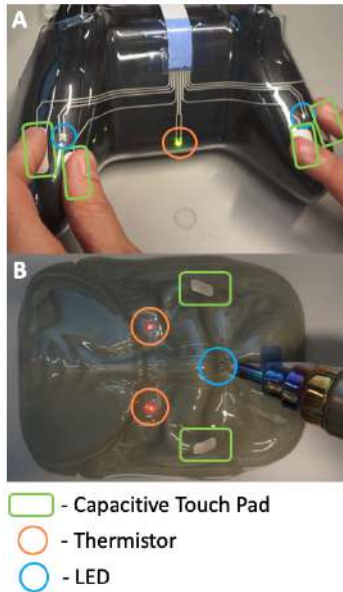


Figure 5: *iMold* enables complex shape objects with sensing/output functionalities. (A) Game controller-skin with grasp sensing using capacitive touch pad and thermistor. (B) Wearable mask translating touch and temperature sensing into LED output.

points will be inserted to the styling curve and the the styling curve becomes smoother and smoother.

Conductivity Failure Detection

During the forming process, the deformation of the 3D formed shape could be dramatic such that the trace passing through the highly deformed regions could have a significant change in conductivity. To understand the effect of the length change (strain) of the trace to the conductivity, we conduct several experiments to assess relationship among trace width, strain and conductivity. With the 2D-to-3D mapping, we compute both of the lengths of the traces in 2D and 3D, and thus obtain the strains of the traces. In practice, if the length change is more than 35% of its original length in 2D, the trace is considered to have high possibility to fail.

Together with the strain-conductivity curve, we have a prediction of the conductivity failure, and will notify the user for possible adjustment. For traces identified as conductivity failure, users could move the traces out of the highly deformed regions to decrease the strain by dragging the control point of the styling curves. Users will continue the adjustment to the traces until they are not identified to have potential conductivity failure. We implemented the proposed conductivity failure detection function together with the interactive trace generation tools and the 2D-to-3D mapping method under our novel computational framework based on C++ programming language and OpenGL library, and allowed user to use it for design and customized electronics functionality fabricated by thermoforming.

Example Usage Scenario

As shown in Figure 5, a user can form complex 3D shapes into electrically functional articles using *iMold*. Whether given geometries of steep slopes or small radius of curva-

tures, proposed software guided IME process can support these without observed experimental failure among out trials. Extending this work to potentially industrial scale is promising since larger printing area and larger 3D molds are widely seen in industry. Furthermore, we ensured compatibility of *iMold* software with standard 3D CAD design files to ensure smooth transition between different design phases.

The examples in Figure 5 show that combination of sensing and output functionalities can be brought into various objects. Here, we integrate capacitive touch sensing through printed conductive pads, temperature sensing using a standard thermistor, and light output using standard LEDs packages.

Conclusion and Future Work

We present *iMold*, a novel software-guided IME process that enables interactive design optimization. We developed a computational design toolkit to perform interactive customization of electronic patterns while optimizing given design with electrical failure detection. Moreover, we developed a full-modified IME process from design, fabrication and components assembly by implementing an automatic surface-mounting process before vacuum forming. Our work potentially benefits people working in IME industry by providing systematic and seamless software-to-process workflow. Our future work will involve fully integrating our software with established IME process and seeking quantitative understanding of how *iMold* facilitates process development of IME.

REFERENCES

- [1] Sun Chemical. 2019. In-Mold Electronic Materials. Retrieved Nov 30, 2019. (Nov. 2019). from

- <https://www.sunchemical.com/product/in-mold-electronic-materials-ime>.
- [2] DuPont. 2019. DuPont In-Mold Electronic Technology. Retrieved Nov 30, 2019. (Nov. 2019). from <https://www.dupont.com/products/in-mold-electronic-technology.html>.
- [3] DuraTech. 2019. IN-MOLD ELECTRONICS (IME). Retrieved Nov 30, 2019. (Nov. 2019). from <https://www.duratech.com/capabilities/ime-in-mold-electronics>.
- [4] Eastprint. 2019. IN-MOLD ELECTRONICS DESIGN & MANUFACTURING AT EASTPRINT, INC. Retrieved Nov 30, 2019. (Nov. 2019). from <https://www.eastprint.com/in-mold-electronics.html>.
- [5] ECM. 2019. Product List. Retrieved Nov 30, 2019. (Nov. 2019). from http://www.conductives.com/new_products.php.
- [6] Ghaffarzadeh, Khasha and Collins, Richard . 2019. *In-Mold Electronics 2019-2029: Technology, Market Forecasts, Players*. Technical Report.
- [7] Pentti Karioja, Jukka-Tapani Mäkinen, Kimmo Keränen, Janne Aikio, Teemu Alajoki, Tuomo Jaakola, Matti Koponen, Antti Keränen, Mikko Heikkinen, Markus Tuomikoski, and others. 2012. Printed hybrid systems. In *Nanosensors, Biosensors, and Info-Tech Sensors and Systems 2012*, Vol. 8344. International Society for Optics and Photonics, 83440G.
- [8] Terho Kololuoma, Mikko Keränen, Timo Kurkela, Tuomas Happonen, Marko Korkalainen, Minna Kehusmaa, Lucia Gomez, Aida Branco, Sami Ihme, Carlos Pinheiro, and others. 2019. Adopting Hybrid Integrated Flexible Electronics in Products: Case-Personal Activity Meter. *IEEE Journal of the Electron Devices Society* (2019).
- [9] Ligang Liu, Lei Zhang, Yin Xu, Craig Gotsman, and Steven J Gortler. 2008. A local/global approach to mesh parameterization. In *Computer Graphics Forum*, Vol. 27. Wiley Online Library, 1495–1504.
- [10] JT Mäkinen, K Keränen, T Alajoki, M Koponen, A Keränen, A Kemppainen, and K Rönkä. 2011. Over-molded electronics and printed hybrid systems. In *SMTA Microelectronic Symposium, Kona*. 18–20.
- [11] Creative Materials. 2019. Conductive Silver Inks. Retrieved Nov 30, 2019. (Nov. 2019). from <http://www.creativematerials.com/products/silver-inks>.
- [12] TactoTek Oy. 2019. TactoTek. Retrieved Nov 30, 2019. (Nov. 2019). from <https://tactotek.com>.
- [13] Christian Schüller, Daniele Panozzo, Anselm Grundhöfer, Henning Zimmer, Evgeni Sorkine, and Olga Sorkine-Hornung. 2016. Computational thermoforming. *ACM Transactions on Graphics (TOG)* 35, 4 (2016), 43.
- [14] Charlie CL Wang. 2004. CyberTape: an interactive measurement tool on polyhedral surface. *Computers & Graphics* 28, 5 (2004), 731–745.
- [15] Yunbo Zhang and Tsz Ho Kwok. 2017. An interactive product customization framework for freeform shapes. *Rapid Prototyping Journal* 23, 6 (2017), 1136–1145.
- [16] Yizhong Zhang, Yiyong Tong, and Kun Zhou. 2016. Coloring 3D printed surfaces by thermoforming. *IEEE transactions on visualization and computer graphics* 23, 8 (2016), 1924–1935.